2024 European Control Conference (ECC)
June 25-28, 2024. Stockholm, Sweden

A novel Newton-based extremum seeking controller for dynamic soaring

Sameer Pokhrel and Sameh A. Eisa, *IEEE member*

***Abstract*—Dynamic soaring is a remarkable flight strategy employed by soaring birds like albatrosses to harness energy from the atmospheric wind gradient. This strategy is so efficient that soaring birds can sustain flight for very long distances without almost flapping their wings. This phenomenon has intrigued researchers across multiple disciplines including biology, physics, and applied mathematics. For aerospace and control engineering researchers, mimicking dynamic soaring means new technologies that contribute to a more sustainable aviation industry. Significant work has been done in the literature to mimic dynamic soaring using optimal control frameworks. However, these approaches have limitations as they are non-real-time, model-dependent, and computationally expensive. Very recently, the authors of this paper introduced a novel autonomous, real-time, and model-free approach for mimicking dynamic soaring utilizing Extremum Seeking Control (ESC) methods. However, the ESC structures used in said emerging approach are sensitive to the curvature of the input-output map of the system. Therefore, in this paper, we propose a Newton-based ESC structure for dynamic soaring that is independent of the input-output map's curvature. This provides a twofold contribution: (1) further solidification that the dynamic soaring problem can be treated as a natural ESC system; and (2) a framework that captures dynamic soaring independent of the input-output map's curvature, which can be particularly useful in cases where the system model is unknown. We verify our real-time results via simulations and comparison with non-real-time powerful optimal control solvers.**

***Index Terms*—Dynamic soaring, Extremum Seeking Control, Newton Method, Real-time Optimization, Biomimicry.**

I. Introduction

The flight exhibited by soaring birds, including but not limited to eagles and albatrosses, through the maneuver known as the "dynamic soaring" has captured the minds, interest, and fascination of scholars from different science and engineering communities. For instance, observations and writings about soaring birds' flight go back to Lord Rayleigh and Leonardo da Vinci [1], [2]. How do these birds fly about 8.5 million kilometers in their life span [3] – which is almost 20 times the distance between Earth and the moon? How do they fly very large distances – over 900 kilometers per day [4] – which seems to exceed by a very large margin the energy they get from their food intake? Indeed, it is a challenge to overstate how interesting and impressive the energy efficiency of soaring birds is.

Dynamic soaring as a phenomenon has been studied for decades – see for example the review papers [5], [6]. In order for soaring birds to perform dynamic soaring, they conduct what can be described as four distinct flight phases: (1) windward climb, (2) high-altitude turn, (3) leeward descent, and (4) low-altitude turn – see Figure 1. Through these distinctive flight phases, the bird covers a significant distance with minimal energy expenditure utilizing the physical property known as "wind shear" [6] taking place when the wind speed varies with altitude, commonly observed above seas and oceans [7]. In addition, it's worth mentioning that the experimental validation of the dynamic soaring flight maneuver has been conducted with albatrosses [8], [9]. Now, if we are able to replicate/mimic the dynamic soaring flight maneuver, substantial technological developments can take place in Unmanned Aerial Vehicles (UAVs), and the enhancement of their endurance, range, energy efficiency, and sustainability; it is simply a miraculous-like perspective that we can fly UAVs almost for free for hundreds of kilometers as soaring birds do!

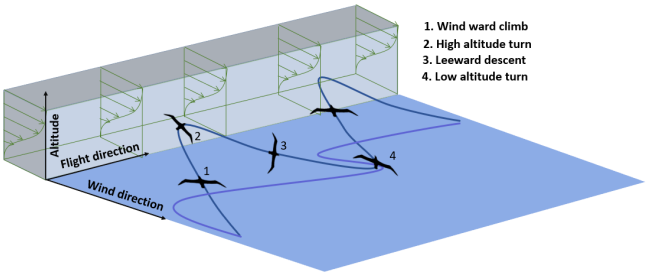

Fig. 1. The dynamic soaring maneuver of an albatross, characterized by four distinct flight phases (1-4) depicted in a dark blue trajectory, observed in the presence of a logistic wind distribution (illustrated in green) above the surface of the ocean.

As a result, decades-long literature has developed mainly in the aeronautical/aerospace and control engineering communities [6] to take us steps closer to the dream of mimicking dynamic soaring by UAVs. Said decades-long literature, discussed in more detail in section II, is almost exclusively dependent on solving the dynamic soaring problem as an optimal control one, through which, we determine the control input signals (e.g., pitch and roll) that if applied by the bird or the mimicking UAV, a successful dynamic soaring maneuver will be achieved. However, very recently, the

This research is funded by the 2023 Office of Research URC Faculty Scholars Research Award at the University of Cincinnati, OH-USA.

Sameer Pokhrel is a PhD student in the Department of Aerospace Engineering and Engineering Mechanics, University of Cincinnati, Ohio, USA (e-mail: pokhresr@mail.uc.edu).

Sameh A. Eisa is an assistant professor in the Department of Aerospace Engineering and Engineering Mechanics, University of Cincinnati, Ohio, USA (e-mail: eisash@ucmail.uc.edu).

authors of this paper have introduced a novel approach to solve the dynamic soaring problem: dynamic soaring can be performed as an extremum seeking system, and the manifestation of the dynamic soaring phenomenon seems to align with the principles of extremum seeking systems in the natural world [10], [11] –discussed in more details in section II. Extremum seeking systems are also control systems [12]–[14] and are often referred to by "ESC." They are (i) model-free as long as measurements of the objective function are obtainable, (ii) real-time, and (iii) not requiring constraints. We succeeded in implementing dynamic soaring using two important structures of ESC systems: the so-called classic ESC structure (see the work of Krstic and Wang in [15], and [12], for more details on the classic structure) and a control-affine ESC structure (see [16]–[22] for more details on control-affine ESC structure, its applications and its relation with averaging). In [10], [23] we showed that dynamic soaring is naturally characterized/mimicked by the classic ESC structure via simulations. We additionally presented a generalized analysis and mathematical derivation, illustrating that dynamic soaring can be interpreted as a control-affine ESC system in [11].

In this paper, we present a novel interpretation of dynamic soaring as a Newton-based ESC system (elaborated further in section III). This novel characterization of dynamic soaring as a Newton-based ESC reaffirms our recent approach in [10], [11], that dynamic soaring is so natural as an ESC system that even a different structure such as Newton-based ESC is also applicable and able to capture the phenomenon. Additionally, using Newton-based ESC brings major advantages, especially to the control engineering side of the problem, by providing an ESC approach that is insensitive to the curvature of the input-output map of the system unlike the ESC structures we introduced in [10], [11]. In section IV, we provide all the details on the design of our control approach and structure. We also provide numerical simulation results using our approach (real-time) and compare them with the powerful optimal control solver (non-real-time) GPOPS2 [24] to demonstrate the effectiveness of our novel Newton-based ESC dynamic soaring approach.

II. Decades-long literature of dynamic soaring vs recent revolutionary extremum seeking approach

As previously discussed in Section I, dynamic soaring has traditionally been formulated in the literature as an optimal control problem, either partially or fully [6], [25]–[29]. However, these formulations are nonlinear, model-dependent, heavily constrained, and non-real-time. Numerical optimizers, such as general purpose optimal control software (GPOPS), inverse dynamics in the virtual domain (IDVD), graphical environment for simulation and optimization (GESOP), Imperial College London optimal control software (ICLOCS), nonlinear programming solver (NPSOL), and advanced launcher trajectory optimization software (ALTOS), have been utilized to generate dynamic soaring trajectories in literature [24], [28]–[31]. These solvers perform computations in non-real-time and can take up to 1000 seconds for one maneuver, depending on factors such as desired accuracy, problem's complexity, and the algorithm used [27]. In some research works [32]–[35], optimal trajectories have been tracked using different controller architectures, such as feed-forward-feedback control, nonlinear control, bio-inspired fuzzy rules, etc. This decades-long trend of the literature of dynamic soaring is depicted in Figure 2.

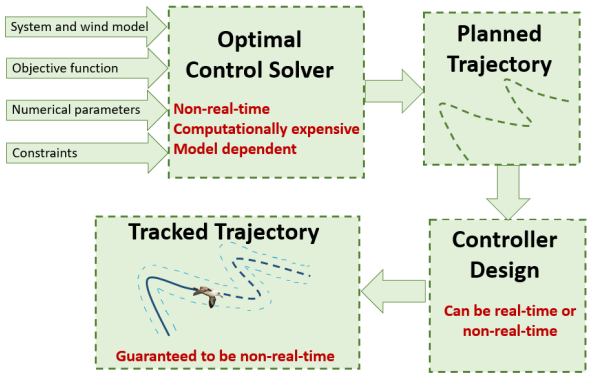

Fig. 2. In the literature, optimal control solvers are commonly used to derive planned trajectories. However, these solvers are non-real-time, computationally expensive, and model-dependent. Following trajectory planning, a controller is employed to ensure the system tracks the trajectory within an acceptable margin of error. Regardless of the chosen controller design, the process remains non-real-time due to the computation involved in trajectory planning. The "Tracked Trajectory" block depicts the tracked and remaining segments of the planned trajectory in solid blue and dashed blue lines, along with the controller's error margin in lighter dashed curves.

On the other hand, as mentioned in Section I, ESC has been shown to be natural to the dynamic soaring problem. It can guide a dynamic system, like an albatross or a mimicking UAV, in real-time towards the highest/lowest point of an objective function without requiring knowledge of its mathematical expression, as long as accurate measurements are available. This feature sets ESC apart from optimal control formulations, making it a powerful alternative approach. Thus, it is motivating to further investigate a controller that is autonomous, model-free, and operates in real-time to address the dynamic soaring problem using measurement via sensors, which is inspired by an albatross that performs dynamic soaring in real time without prior knowledge of wind profiles or mathematical representations of the objective function by sensing its surroundings (measurement via sensors) – see for example these studies which conclude that albatrosses nostrils sense wind speed [36], [37].

Before discussing our novel solution approach using Newton-based ESC for dynamic soaring, we will first provide a brief overview of the wind shear models, flight dynamics models, essential bounds/constraints, and problem formulation as presented in the literature. This overview sets the context and serves as the operational foundation for the numerical optimizer used for comparison in Section IV.

A. Wind shear model

Wind shear refers to the fluctuation in wind speed across a localized region in the atmosphere. It plays an important role

in facilitating energy harvesting through dynamic soaring [6], [25]. Hence, having a proper wind shear model is important for optimal control techniques that are model-dependent. Usually, in literature, vertical wind shear is assumed. That is because, at sea level, the wind speed is almost negligible, but it gradually rises with altitude. To simulate this, numerous models have been employed in previous research works on optimal control of dynamic soaring [6]. In [10], both logarithmic and logistic wind profiles were used to analyze dynamic soaring as an ESC problem. In this work, we only consider a logistic wind profile provided by (1) as

$$W(z) = \frac{W_0}{1 + e^{-(z - z_m)/\delta}}. \tag{1}$$

This wind model has three main parameters: free stream wind velocity W_0, the thickness of the shear layer denoted by δ, and the altitude corresponding to the middle of the shear layer, denoted by z_m. The corresponding wind profile is shown in Figure 3.

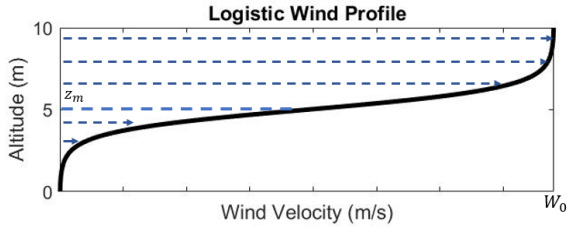

Fig. 3. A logistic wind profile with free stream wind velocity $W_0 = 7.8\, m/s$, shear layer thickness $\delta = 2/3\, m$, and the altitude $z_m = 5\, m$.

B. Flight dynamics model

The optimal control literature for dynamic soaring has featured models with three or six degrees of freedom, as evident in studies such as [6], [25], [28], [29], [38]. However, the use of six degrees of freedom models (see [38]), may not provide substantial accuracy improvements relative to computational costs, as pointed out in [6]. Thus, a point-mass model is considered to represent either an albatross or a mimicking UAV, with no thrust component similar to the ones used in [10], [11]:

$$\begin{aligned}
\dot{x} &= V\cos\gamma\cos\psi,\\
\dot{y} &= V\cos\gamma\sin\psi - W,\\
\dot{z} &= V\sin\gamma,\\
m\dot{V} &= -D - mg\sin\gamma + m\dot{W}\cos\gamma\sin\psi,\\
mV\dot{\gamma} &= L\cos\phi - mg\cos\gamma - m\dot{W}\sin\gamma\sin\psi,\\
mV\dot{\psi}\cos\gamma &= L\sin\phi + m\dot{W}\cos\psi.
\end{aligned} \tag{2}$$

The frame of reference taken here is East, North, and Up denoted by (i, j, k) in Figure 4. In this notation, the roll angle is denoted by ϕ, and the heading angle, measured between the projection of velocity V in the ij-plane and i, is denoted by ψ. Similarly, the flight path angle, represented by γ, is the angle between velocity V and the ij-plane, considering a positive orientation when the nose is elevated. The wind is

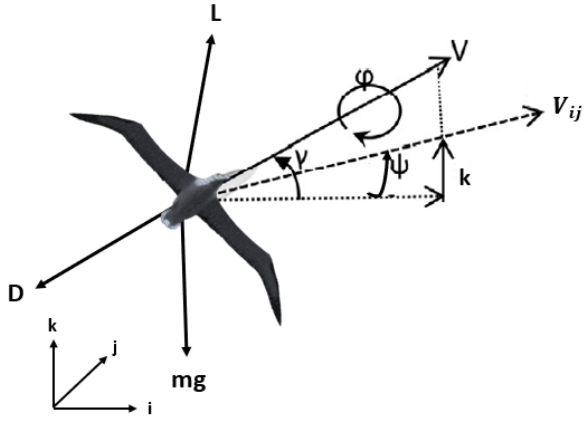

Fig. 4. The frame of reference, aerodynamic angles, and the aerodynamic forces acting on soaring birds like albatrosses or mimicking UAVs.

characterized by a density ρ, velocity W, and shear gradient $\dot{W}$. It consistently blows in a North-to-south direction, contributing only to horizontal wind components. Additionally, the angles and speed are expressed in the relative reference frame of the wind, while the spatial coordinates (x, y, z) are expressed in the Earth's fixed frame. The aerodynamic forces, lift (L) and drag (D), are described as follows.

$$\begin{aligned}
L &= \frac{1}{2}\rho V^2 S C_L,\\
D &= \frac{1}{2}\rho V^2 S C_D,
\end{aligned} \tag{3}$$

where the lift coefficient is represented by C_L, and the drag coefficient, denoted as C_D, is determined through $C_D = C_{D0} + KC_L^2$. Here, C_{D0} is the zero-lift drag coefficient, while K is the coefficient of induced drag. Table I provides the parameters associated with the albatross and the environmental conditions.

Parameter	Value
m	8.5 kg
S	0.65 m^2
C_{D0}	0.033
K	0.019
ρ	1.225 kg/m^3
g	9.8 m/s^2
W_0	7.8 m/s
δ	2/3 m
z_m	5 m

TABLE I
PARAMETERS RELATED TO THE ALBATROSS AND THE ENVIRONMENT USED IN THIS STUDY.

C. Optimal control problem formulation

In the optimal control formulation commonly used for studying dynamic soaring in existing literature [6], the state vector $\boldsymbol{x}(t)$ and the control vector $\boldsymbol{u}(t)$ are defined as follows:

$$\begin{aligned}
\boldsymbol{x}(t) &= [x, y, z, V, \gamma, \psi],\\
\boldsymbol{u}(t) &= [C_L, \phi],
\end{aligned} \tag{4}$$

where the symbols have the usual meaning as described earlier in subsection II-B. The nonlinear system, incorporating the flight dynamics from (2) and the wind model described in (1), can be expressed as follows:

$$\dot{\boldsymbol{x}}(t) = \boldsymbol{f}(\boldsymbol{x}(t), \boldsymbol{u}(t)). \tag{5}$$

The primary objective is to maximize the performance index, denoted as $J = g(\boldsymbol{x}; \dot{W})$, which generally depends on both the wind shear/gradient and the state vector. Various choices for the objective function in dynamic soaring are available, as outlined in [6]. For this study, we focus on the most relevant objective function: maximum energy gain

$$J = \max(Energy)_{gain}, \tag{6}$$

with its expression provided in subsection IV-C. The bird's final state after completing a cycle depends on the chosen dynamic soaring mode—basic, loiter, or travel modes, as explained in [6]. In loiter mode, the final position must exactly match the initial coordinates. In travel mode, the post-maneuver position is partially fixed, whereas in basic mode, there are no constraints on the final position after the maneuver—it's unconstrained with respect to position. In this study, the basic mode is selected, leading to the following boundary constraints:

$$[z, V, \gamma, \psi]{t_f}^T = [z + \Delta z, V, \gamma, \psi]{t_0}^T, \tag{7}$$

where t_0 and t_f symbolize the initial and final times, respectively, while Δz denotes the net change in altitude following the completion of the dynamic soaring cycle. Similarly, path constraints for states and control inputs throughout the dynamic soaring cycle are provided in (8):

$$\begin{aligned} V_{\min} < V < V_{\max}, \psi_{\min} < \psi < \psi_{\max}, \\ \gamma_{\min} < \gamma < \gamma_{\max}, x_{\min} < x < x_{\max}, \\ y_{\min} < y < y_{\max}, z_{\min} < z < z_{\max}, \\ \phi_{\min} < \phi < \phi_{\max}, C_{L_{\min}} < C_L < C_{L\max}. \end{aligned} \tag{8}$$

III. Newton-based extremum seeking control and its advantages

Extremum seeking control (ESC) is an adaptive and model-free control technique that was introduced almost a century ago to stabilize a dynamical system around the extremum (maximum or minimum) point of an objective function, that may not be known expression-wise [12], [14]. Its applications extend across a wide range of disciplines, as explained in [12]. With particular relevance to our efforts in bringing this technique to bio-inspiration/mimicry of soaring birds in [10], [11], we note that ESC structures (both classic and control-affine structures) have found appealing applications in decoding biological phenomena and bio-mimicry. For instance, Cochran et al. [39] succeeded in utilizing model-free ESC for source seeking by fish. Similarly, ESC has been used in the bio-mimicry of motion of the bacterium Escherichia coli (*E. Coli*) [40] and sea urchin sperm cells [41]. One important thing to note is that all of the above-mentioned references used perturbation-based ESC (classic and control-affine).

The effectiveness of perturbation-based (sometimes called gradient-based) ESCs is greatly impacted by the curvature of the underlying map when using structures based on gradient descent adaptation. Such structures that realize the gradient by perturbing the feedback measurement of the objective function, necessitate substantial tuning efforts to ensure stability across a wide range of operating conditions. In contrast, Newton-based methods remain unaffected by map curvature and prove valuable in scenarios where the system model and Hessian are unknown, as is the case in ESC systems. Moase, Manzie, and Brear proposed a Newton-like algorithm for ESC in the late 2000s, which estimates the gradient and Hessian of the map for a single-input system using a Newton-like algorithm [42], [43]. A general framework for estimating higher order derivatives when the cost function itself is unknown is described in [44]. However, finding the inverse of the Hessian can be challenging in multivariable systems. To address this, Ghaffari et al. introduced a multi-variable Newton-based ESC [45]. Newton-based ESCs have since been extended to stochastic systems [46], higher derivatives of unknown maps [47], and various applications such as power optimization for photovoltaic microconverters [48]. Recently, higher-order Lie brackets approximation techniques have been used to extend the Newton-based method to control-affine ESCs [20], [49]. Figure 5 depicts the basic scheme of the Newton-based ESC, where the parameter θ is updated to reach the maximum/minimum of the objective function J. First, a sinusoidal signal $a\sin(\omega t)$ is added to

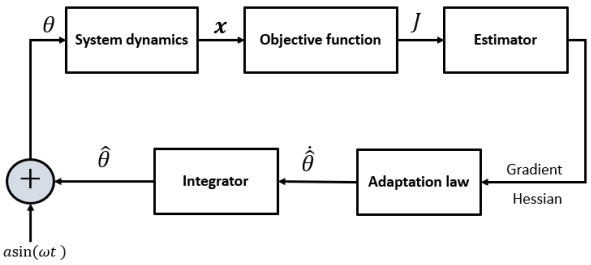

Fig. 5. The basic scheme of a Newton-based ESC involves the addition of a perturbation signal to the parameter $\hat{\theta}$, which is then input into the system dynamics. The objective function is measured, and an estimator is employed to estimate both the gradient and Hessian. The adaptation law, utilizing a Newton-like method, along with an integrator, is employed to update the parameter $\hat{\theta}$.

the initial estimate of the parameter $\hat{\theta}$, where a and ω denote the amplitude and frequency of the signal, respectively. Subsequently, the resulting value of θ is input into the system dynamics, and the objective function J is measured. It is essential to highlight that only the measurement of J is required, and the explicit mathematical form of the objective function is not needed. An estimator is used to derive the gradient and Hessian values from the measured objective function J. These values are then utilized in an adaptation law based on the Newton-like method to update $\hat{\theta}$. The outcome of this update determines whether the estimation of θ should increase or decrease. The guess value of the parameter $\hat{\theta}$ is

then updated through an integrator.

IV. A NOVEL NEWTON-BASED EXTREMUM SEEKING CONTROL FOR DYNAMIC SOARING

In this section, we present the rationale behind connecting Newton-based extremum seeking controller (ESC) with dynamic soaring and describe the framework of our proposed Newton-based ESC model for dynamic soaring that encompasses both trajectory planning and tracking. Additionally, we present the results of simulations conducted on our model and compare them to those obtained using a powerful optimal method mentioned in the literature.

A. Reasoning for the use of Newton-based extremum seeking for dynamic soaring

The application of Extremum Seeking Control (ESC) to address the dynamic soaring problem was introduced in [10], [11] by the authors of this paper, representing the first real-time implementable approach for dynamic soaring since it was initially discussed by Lord Rayleigh [2]. In these works, a hypothesis was put forth, suggesting a parallelism between ESC and dynamic soaring. It was proposed that the variation or perturbation in the bird's pitching and rolling actions corresponds to the modulation step in an ESC. Additionally, sensing changes in the surrounding environment, such as wind, height, and velocity, is analogous to measuring the objective function, while updating the rolling/pitching action based on feedback is comparable to the parameter update step. A proof of concept for this hypothesis was provided through mathematical analysis and simulations, with comparisons against results obtained using a powerful optimal control solver [10], [11]. However, the convergence rate and stability of perturbation-based ESCs employed in these works are sensitive to the curvature of the input-output map, given the use of the gradient descent adaptation algorithm. As a result, if operating conditions vary significantly, the system requires retuning. Furthermore, for the dynamic soaring problem, no prior knowledge of the system model or the expression of the objective function is assumed. Therefore, a method that is independent of map curvature is highly desirable, especially from a control engineering standpoint. The Newton-based ESC satisfies these criteria and addresses the shortcomings of perturbation-based ESCs. Thus, we use it for this research work.

B. Structure of Newton-based ESC for dynamic soaring

In section III, we introduced a general structure of the Newton-based ESC, which was illustrated in Figure 5. To tailor this structure to solve the dynamic soaring problem, we will customize it as follows. For system dynamics, we assume it to be the albatross/mimicking-UAV flight dynamics. For the simulation we conduct later, we consider the model given in (2). It's worth noting that in a real ESC implementation, having a model is not necessary, as long as objective function measurements are accessible. Similar to the rationale and sense of [10], [11], we adopt the scenario with the constant C_L to obtain a single-input single-output (SISO) system with rolling action/control ϕ as the sole input, given that this work is introductory results. Since ϕ is the input to the system dynamics model, we set the parameter θ to be $\theta = \phi$. This choice implies that the rolling action/control becomes the parameter optimized to either maximize (or minimize) the objective function of the system. The single output is now the objective function J, as expressed in (6), and it is assumed to depend on the states and the wind shear/gradient, represented as $J = g(\boldsymbol{x}, \dot{W})$. This completes the customization of the Newton-based ESC system for the dynamic soaring as a maximization problem, and the customized structure is provided in Figure 6. As done in [10], [11], the objective function corresponding to specific energy gain can be derived by taking the derivative of specific total energy $e = z + \frac{V^2}{2g}$, with respect to time as follows

$$\dot{e} = \dot{z} + \frac{V\dot{V}}{g} \tag{9}$$

$$= V sin\gamma + \frac{V}{g}[-D - g\sin\gamma - \dot{W}\cos\gamma\sin\psi] \tag{10}$$

$$= -\frac{DV}{g} - \frac{V\dot{W}\cos\gamma\sin\psi}{g}. \tag{11}$$

As we can see in (11), the term $-V\dot{W}\cos\gamma\sin\psi/g$ is the metric for determining energy gain from the wind and is adopted as the performance index. A similar objective function was studied and used in [10]. Although assuming complete knowledge of the behavior of the objective function is challenging, we assume here that the objective function satisfies the required mathematical conditions (e.g., smoothness, convexity, unique optimum, etc.), similar to the approach in [42], [43], and as utilized in our previous works [10], [11]. The rest of the structure in Figure 6 is similar to that provided in Figure 5. We use the Kalman filter as the estimator to estimate the gradient and Hessian of the objective function. Finally, we use an adaptation law that utilizes a Newton-like method to update the value of the nominal parameter $\hat{\phi}$. Next, we describe the adaptation law and Kalman filter in detail.

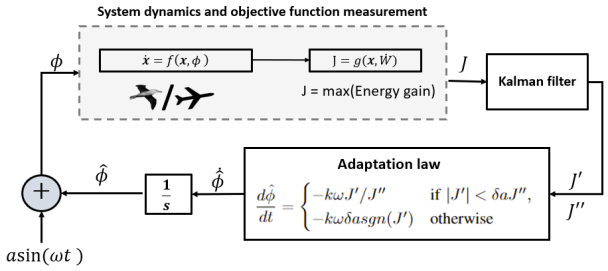

Fig. 6. A novel Newton-based ESC system for the dynamic soaring problem. This structure is similar to that in Figure 5 but with the roll angle (ϕ) as a control input, (2) as system dynamics, maximum energy gain as the objective function, and Kalman filter as the estimator.

Adaptation law. The adaptation law used in this study is similar to that presented in [42] and is based on a Newton-like method, as shown in equation (12):

$$\frac{d\hat{\phi}}{dt} = \begin{cases} -k\omega J'/J'' & \text{if } |J'| < \delta a J'', \\ -k\omega\delta a sgn(J') & \text{otherwise.} \end{cases} \tag{12}$$

The dimensionless constants δ and k, the gradient and Hessian values (J' and J''), and information of perturbation signal are used to progress the control parameter $\hat{\phi}$ according to the Newton-like method when $|J'| < \delta a J''$, and as per the sign of the gradient otherwise. This approach offers several advantages, including the avoidance of the point of inflection when $J'' = 0$ and the saturation of the maximum rate of change for $\hat{\phi}$ to $kw\delta a$, leading to more desirable results.

Kalman Filter. For the Kalman filter, we use similar concepts used in [50], [51]. Let us consider a system with no dynamics with input $\hat{\phi}$ and output $\hat{J}$. Now, using Taylor series expansion of $\hat{J}$ about $\hat{\phi}$ is

$$J = \hat{J} + \hat{J}' a \sin(\omega t) + 1/2 \hat{J}'' a^2 \sin^2(\omega t) + h, \tag{13}$$

where h represents higher-order terms, a, ω represent amplitude and frequency of perturbation signal. Now, to estimate the gradient and Hessian, let us define the state variables $\bar{x}$ as given in (14):

$$\bar{x} = \begin{bmatrix} \hat{J} + 1/4 a^2 \hat{J}'' \\ \hat{J}' a \sin(\omega t) \\ \hat{J}' a cos(\omega t) \\ \hat{J}'' a^2 \sin(2\omega t) \\ \hat{J}'' a^2 \cos(2\omega t) \end{bmatrix}, A = \begin{bmatrix} 0 & 0 & 0 & 0 & 0 \\ 0 & 0 & 1 & 0 & 0 \\ 0 & -1 & 0 & 0 & 0 \\ 0 & 0 & 0 & 0 & 2 \\ 0 & 0 & 0 & -2 & 0 \end{bmatrix} \tag{14}$$

By assuming that the change in $\hat{\phi}$ is slower compared to the dither signal, we get the dynamical equation as

$$\dot{\bar{x}} = A\bar{x} + \Omega, \tag{15}$$

where A is given in (14) and Ω represents unmodeled dynamics and is assumed to be Gaussian with zero mean and covariance $\boldsymbol{Q}$. Now, by assuming the the higher-order terms (h) as Gaussian measurement noise $\nu(t) \sim N(0, r)$, we get from (13):

$$J = C\bar{x} + \nu, \tag{16}$$

where $C = [1, 1, 0, 0, -1/4]$. Thus, (15) and (16) constitute the state update and measurement update equation for the Kalman filter. Now, the gradient and Hessian can be extracted from the states of the Kalman filter using the following equations:

$$a\hat{J}' = C'\bar{x};\ C' = [0, \sin(\omega t), \cos(\omega t), 0, 0] \tag{17}$$

$$a^2\hat{J}'' = C''\hat{J};\ C'' = [0, 0, 0, \sin(2\omega t), \cos(2\omega t)] \tag{18}$$

Remark. Apart from our novel contribution using Newton-based ESC for dynamic soaring, we also tried to identify which kind of estimator works best for this problem, as other estimators like Luenberger observer can be found in the literature. We found that the gain value for the Luenberger observer is difficult to get and also the unmodeled dynamics are ignored. On the other hand, for the Kalman Filter, the unmodeled dynamics are modeled as noise, and the algorithm itself has a method to get the optimal gain. In addition, we found that the result using the Kalman Filter is better when compared to the Luenberger observer. Thus, the Kalman filter is chosen as the estimator. Of note, the Kalman filter can be found in the literature of Newton-based ESC [52].

C. Simulations and comparative results

In this subsection, we perform simulations for the newly proposed Newton-based ESC tailored for dynamic soaring. Additionally, we compare the simulation results with solutions obtained from GPOPS2 [24], an optimization software compatible with MATLAB®, utilizing hp-adaptive Gaussian quadrature collocation methods and sparse nonlinear programming. In these simulations, a logistic wind profile is used for wind modeling, and the objective function is defined as the energy gain, expressed as $J = -\frac{V\dot{W}\cos\gamma\sin\psi}{g}$, as provided in (11). Table I lists the parameters associated with the albatross and its environment. It is crucial to emphasize that the explicit expressions for the objective function, system dynamics model, wind model, and constraints are not necessary for ESC implementation; however, we include them for the sake of comparison with GPOPS2. Furthermore, for ESC, we use a modulating signal in the form of $a\sin(\omega t)$, where $a = 1$ and $\omega = 1$. For the adaptation law, we set $k = 1$ and $\delta = 1$. We set the initial state as $[-16, 15, 10, 14, -0.66, -0.135]$ and apply a constant value of $C_L = 1.5$. Finally, for the Kalman filter, we set the initial state as $\bar{x}_0 = [0.1, 0.1, 0.1, 0.1, 0.1]$, with $Q = 0.01 I_{5\times5}$ and $R = 0.01$.

Next, we discuss the outcomes of our simulation applying the novel Newton-based ESC and GPOPS2. The key measure of the success of our implementation is evident in Figure 7, where energy neutrality (near-neutrality) is achieved—a fundamental characteristic of dynamic soaring. Figure 7 shows the comparison of potential energy (PE), kinetic energy (KE), and total energy (TE) obtained using both Newton-based ESC and GPOPS2 during a cycle of dynamic soaring. It is

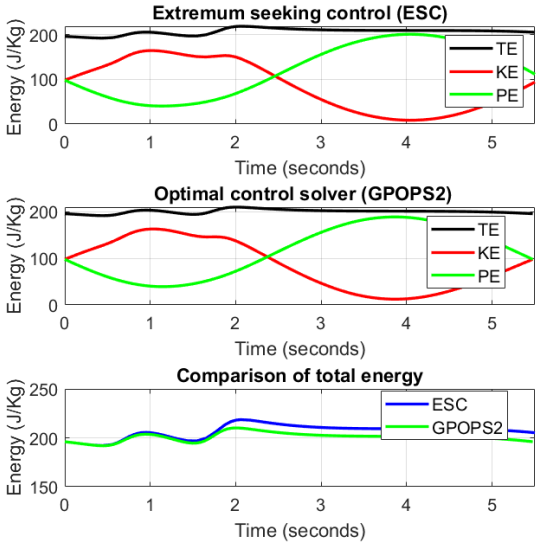

Fig. 7. Comparison of kinetic energy (KE), potential energy (PE), total energy (TE) obtained during a single cycle of dynamic soaring using Newton-based ESC and GPOPS2.

noteworthy that the total energy is nearly constant in both approaches, i.e., the energy is traded off between kinetic and

potential without any or with minimum drag loss. Figure 8 illustrates the comparison between 3D trajectories, while Figure 9 depicts the plot for states and control input vs time obtained using both methods. The outcomes from both methods are quite similar and can be compared: a model-free, real-time, no-constraints Newton-based ESC vs. model-dependent, non-real-time, heavily-constrained GPOPS2.

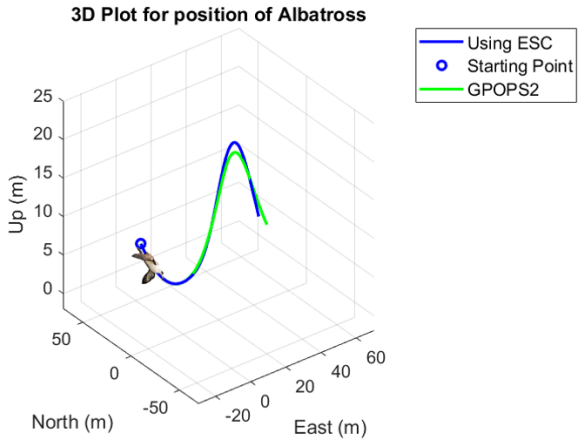

Fig. 8. Comparison of 3D trajectories during a cycle of dynamic soaring obtained using Newton-based ESC and GPOPS2.

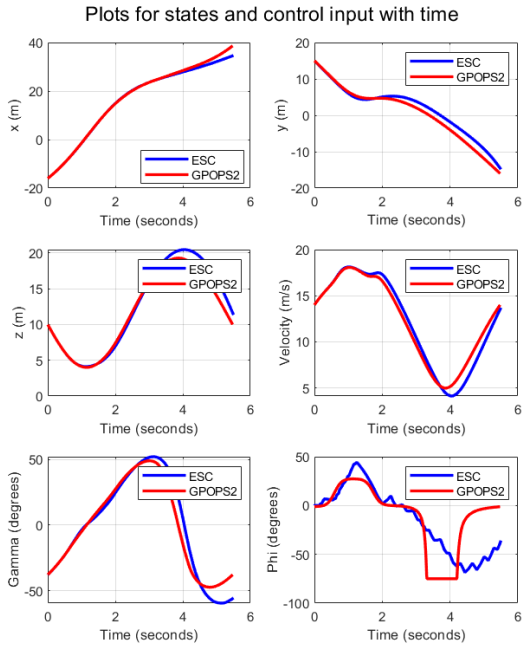

Fig. 9. Comparison of states and control inputs during a cycle of dynamic soaring using Newton-based ESC and GPOPS2.

V. Conclusion

Dynamic soaring is a fascinating phenomenon that has captivated researchers and engineers for many years, with the potential to revolutionize the aviation industry. However, dynamic soaring has been traditionally studied as an optimal control problem that is model-dependent, non-real-time, and heavily constrained [6]. This decades-long approach is severely limiting to a better understanding of dynamic soaring and its applicability. To overcome these issues, an Extremum Seeking Control (ESC) approach has been proposed very recently by the authors of this paper in [10], [11] as a more natural and descriptive way to study and mimic dynamic soaring as it provides a model-free, real-time, no-constraints, and sensing/measurement-based approach – hypothetically inline with what soaring birds do. The Newton-based ESC approach introduced in this paper further solidifies the potential of the ESC approach proposed by the authors [10], [11] breaking away from the decades-long optimal control approach in literature. Additionally, the proposed Newton-based ESC is particularly useful for the control engineering side of the problem when the system model and the objective function curvature are unknown. The simulation results suggest that an important feature of the dynamic soaring phenomenon, near-constant total energy, is captured by the Newton-based ESC which by design is independent of the input-output map's curvature. Similarly, the states and the trajectory obtained using Newton-based ESC are comparable to that obtained in non-real-time via a powerful optimal control solver.

References

[1] P. L. Richardson, "Leonardo da vinci's discovery of the dynamic soaring by birds in wind shear," *Notes and Records: the Royal Society journal of the history of science*, vol. 73, no. 3, pp. 285–301, 2019.

[2] L. Rayleigh, "The soaring of birds," *Nature*, vol. 27, no. 701, pp. 534–535, 1883.

[3] H. Weimerskirch, Y. Cherel, K. Delord, A. Jaeger, S. C. Patrick, and L. Riotte-Lambert, "Lifetime foraging patterns of the wandering albatross: life on the move!" *Journal of Experimental Marine Biology and Ecology*, vol. 450, pp. 68–78, 2014.

[4] P. Jouventin and H. Weimerskirch, "Satellite tracking of wandering albatrosses," *Nature*, vol. 343, no. 6260, pp. 746–748, 1990.

[5] A. Mohamed, G. K. Taylor, S. Watkins, and S. P. Windsor, "Opportunistic soaring by birds suggests new opportunities for atmospheric energy harvesting by flying robots," *Journal of the Royal Society Interface*, vol. 19, no. 196, p. 20220671, 2022.

[6] I. Mir, S. A. Eisa, and A. Maqsood, "Review of dynamic soaring: technical aspects, nonlinear modeling perspectives and future directions," *Nonlinear Dynamics*, vol. 94, pp. 3117–3144, 2018.

[7] P. L. Richardson, "How do albatrosses fly around the world without flapping their wings?" *Progress in Oceanography*, vol. 88, no. 1-4, pp. 46–58, 2011.

[8] G. Sachs, J. Traugott, A. Nesterova, and F. Bonadonna, "Experimental verification of dynamic soaring in albatrosses," *Journal of Experimental Biology*, vol. 216, no. 22, pp. 4222–4232, 2013.

[9] Y. Yonehara, Y. Goto, K. Yoda, Y. Watanuki, L. C. Young, H. Weimerskirch, C.-A. Bost, and K. Sato, "Flight paths of seabirds soaring over the ocean surface enable measurement of fine-scale wind speed and direction," *Proceedings of the National Academy of Sciences*, vol. 113, no. 32, pp. 9039–9044, 2016.

[10] S. Pokhrel and S. A. Eisa, "A novel hypothesis for how albatrosses optimize their flight physics in real-time: an extremum seeking model and control for dynamic soaring," *Bioinspiration & Biomimetics*, vol. 18, no. 1, p. 016014, 2022.

[11] S. A. Eisa and S. Pokhrel, "Analyzing and mimicking the optimized flight physics of soaring birds: A differential geometric control and extremum seeking system approach with real time implementation," *SIAM Journal on Applied Mathematics*, pp. S82–S104, 2023.

[12] K. B. Ariyur and M. Krstic, *Real-time optimization by extremum-seeking control*. John Wiley & Sons, 2003.

[13] A. Scheinker and M. Krstić, *Model-free stabilization by extremum seeking*. Springer, 2017.

[14] Y. Tan, W. Moase, C. Manzie, D. Nešić, and I. Mareels, "Extremum seeking from 1922 to 2010," in *Proceedings of the 29th Chinese Control Conference*, 2010, pp. 14–26.

[15] M. Krstić and H.-H. Wang, "Stability of extremum seeking feedback for general nonlinear dynamic systems," *Automatica*, vol. 36, no. 4, pp. 595–601, 2000.

[16] H.-B. Dürr, M. S. Stanković, C. Ebenbauer, and K. H. Johansson, "Lie bracket approximation of extremum seeking systems," *Automatica*, vol. 49, no. 6, pp. 1538–1552, 2013.

[17] S. Pokhrel and S. A. Eisa, "Control-affine extremum seeking control with attenuating oscillations: A lie bracket estimation approach," in *2023 Proceedings of the Conference on Control and its Applications (CT)*. SIAM, 2023, pp. 133–140.

[18] ——, "Gradient and lie bracket estimation of extremum seeking systems: A novel geometric-based kalman filter and relaxed time-dependent stability condition," *International Journal of Control, Automation and Systems*, vol. 21, no. 12, pp. 3839–3849, 2023.

[19] S. Pokhrel, A. A. Elgohary, and S. Eisa, "Extremum seeking by multi-agent vehicles and uavs with no steady state oscillation using a geometric-based kalman filtering," in *AIAA SCITECH 2024 Forum*, 2024, p. 0724.

[20] S. Pokhrel and S. A. Eisa, "Higher order lie bracket approximation and averaging of control-affine systems with application to extremum seeking," *arXiv preprint arXiv:2310.07092*, 2023.

[21] S. Bajpai, A. A. Elgohary, and S. A. Eisa, "Model-free source seeking by a novel single-integrator with attenuating oscillations and better convergence: Robotic experiments," *arXiv preprint arXiv:2311.04330*, 2023.

[22] B. Moidel, A. A. Elgohary, S. Bajpai, and S. Eisa, "Reintroducing the formation flight problem via extremum seeking control," in *AIAA SCITECH 2024 Forum*, 2024, p. 2317.

[23] S. Pokhrel and S. Eisa, "Extremum seeking in nature: Examination of soaring birds flights maneuver," in *AIAA SCITECH 2023 Forum*, 2023, p. 2239.

[24] M. A. Patterson and A. V. Rao, "Gpops-ii: A matlab software for solving multiple-phase optimal control problems using hp-adaptive gaussian quadrature collocation methods and sparse nonlinear programming," *ACM Transactions on Mathematical Software*, vol. 41, no. 1, oct 2014.

[25] G. D. Bousquet, M. S. Triantafyllou, and J.-J. E. Slotine, "Optimal dynamic soaring consists of successive shallow arcs," *Journal of The Royal Society Interface*, vol. 14, no. 135, p. 20170496, 2017.

[26] I. Mir, S. A. Eisa, H. Taha, A. Maqsood, S. Akhtar, and T. U. Islam, "A stability perspective of bioinspired unmanned aerial vehicles performing optimal dynamic soaring," *Bioinspiration & Biomimetics*, vol. 16, no. 6, p. 066010, 2021.

[27] I. Mir, A. Maqsood, S. A. Eisa, H. Taha, and S. Akhtar, "Optimal morphing–augmented dynamic soaring maneuvers for unmanned air vehicle capable of span and sweep morphologies," *Aerospace Science and Technology*, 2018.

[28] Y. J. Zhao, "Optimal patterns of glider dynamic soaring," *Optimal control applications and methods*, vol. 25, no. 2, pp. 67–89, 2004.

[29] G. Sachs, "Minimum shear wind strength required for dynamic soaring of albatrosses," *Ibis*, vol. 147, no. 1, pp. 1–10, 2005.

[30] G. Sachs and O. da Costa, "Optimization of dynamic soaring at ridges," in *AIAA Atmospheric flight mechanics conference and exhibit*, 2003, p. 5303.

[31] G. Sachs and M. Mayrhofer, "Shear wind strength required for dynamic soaring at ridges," *Technical Soaring*, vol. 25, no. 4, pp. 209–215, 2001.

[32] J. J. Bird, J. W. Langelaan, C. Montella, J. Spletzer, and J. L. Grenestedt, "Closing the loop in dynamic soaring," in *AIAA Guidance, Navigation, and Control Conference*, 2014, p. 0263.

[33] C. Gao and H. H. Liu, "Dubins path-based dynamic soaring trajectory planning and tracking control in a gradient wind field," *Optimal Control Applications and Methods*, vol. 38, no. 2, pp. 147–166, 2017.

[34] R. Barate, S. Doncieux, and J.-A. Meyer, "Design of a bio-inspired controller for dynamic soaring in a simulated unmanned aerial vehicle," *Bioinspiration & biomimetics*, vol. 1, no. 3, p. 76, 2006.

[35] Z. Li and J. W. Langelaan, "Parameterized trajectory planning for dynamic soaring," in *AIAA Scitech 2020 Forum*, 2020, p. 0856.

[36] C. Pennycuick, "Information systems for flying animals," *Theoretical Ecology Series*, vol. 5, pp. 305–331, 2008.

[37] M. d. L. Brooke and J. Vickery, "Gusts keep albatrosses aloft," *Trends in Ecology & Evolution*, vol. 17, no. 6, p. 253, 2002.

[38] N. Akhtar, A. K. Cooke, and J. F. Whidborne, "Positioning algorithm for autonomous thermal soaring," *Journal of aircraft*, vol. 49, no. 2, pp. 472–482, 2012.

[39] J. Cochran, E. Kanso, S. D. Kelly, H. Xiong, and M. Krstic, "Source seeking for two nonholonomic models of fish locomotion," *IEEE Transactions on Robotics*, vol. 25, no. 5, pp. 1166–1176, 2009.

[40] S.-J. Liu and M. Krstic, "Stochastic source seeking for nonholonomic unicycle," *Automatica*, vol. 46, no. 9, pp. 1443–1453, 2010.

[41] M. Abdelgalil, Y. Aboelkassem, and H. Taha, "Sea urchin sperm exploit extremum seeking control to find the egg," *Physical Review E*, vol. 106, no. 6, p. L062401, 2022.

[42] W. H. Moase, C. Manzie, and M. J. Brear, "Newton-like extremum-seeking part i: Theory," in *Proceedings of the 48h IEEE Conference on Decision and Control (CDC) held jointly with 2009 28th Chinese Control Conference*. IEEE, 2009, pp. 3839–3844.

[43] ——, "Newton-like extremum-seeking for the control of thermoacoustic instability," *IEEE Transactions on Automatic Control*, vol. 55, no. 9, pp. 2094–2105, 2010.

[44] D. Nesić, Y. Tan, W. H. Moase, and C. Manzie, "A unifying approach to extremum seeking: Adaptive schemes based on estimation of derivatives," in *49th IEEE conference on decision and control (CDC)*. IEEE, 2010, pp. 4625–4630.

[45] A. Ghaffari, M. Krstić, and D. Nešić, "Multivariable newton-based extremum seeking," *Automatica*, vol. 48, no. 8, pp. 1759–1767, 2012.

[46] S.-J. Liu and M. Krstic, "Newton-based stochastic extremum seeking," *Automatica*, vol. 50, no. 3, pp. 952–961, 2014.

[47] D. Rušiti, T. R. Oliveira, G. Mills, and M. Krstić, "Newton-based extremum seeking for higher derivatives of unknown maps with delays," in *2016 IEEE 55th Conference on Decision and Control (CDC)*. IEEE, 2016, pp. 1249–1254.

[48] A. Ghaffari, M. Krstić, and S. Seshagiri, "Power optimization for photovoltaic microconverters using multivariable newton-based extremum seeking," *IEEE Transactions on Control Systems Technology*, vol. 22, no. 6, pp. 2141–2149, 2014.

[49] C. Labar, E. Garone, M. Kinnaert, and C. Ebenbauer, "Newton-based extremum seeking: A second-order lie bracket approximation approach," *Automatica*, vol. 105, pp. 356–367, 2019.

[50] D. F. Chichka, J. L. Speyer, C. Fanti, and C. G. Park, "Peak-seeking control for drag reduction in formation flight," *Journal of Guidance, Control, and Dynamics*, vol. 29, no. 5, pp. 1221–1230, 2006.

[51] D. Chichka, J. Speyer, and C. Park, "Peak-seeking control with application to formation flight," in *Proceedings of the 38th IEEE Conference on Decision and Control (Cat. No.99CH36304)*, vol. 3, 1999, pp. 2463–2470 vol.3.

[52] H. Wang, M. Hu, Y. Tian, I. Simeonov, L. Kabaivanova, and N. Christov, "Kalman filter based newton extremum seeking control for maximum gases production rates of anaerobic digestion process," *Information Technology and Control*, vol. 49, no. 4, pp. 455–463, 2020.